THE JOURNAL OF PHYSICAL CHEMISTRY C

Article

pubs.acs.org/JPCC

Photocatalytic Water Oxidation on $BiVO_4$ with the Electrocatalyst as an Oxidation Cocatalyst: Essential Relations between Electrocatalyst and Photocatalyst

Donge Wang,[†,‡] Rengui Li,[†,‡] Jian Zhu,[†,‡] Jingying Shi,[†] Jingfeng Han,[†,‡] Xu Zong,[†] and Can Li*[,†]

[†]State Key Laboratory of Catalysis, Dalian Institute of Chemical Physics, Chinese Academy of Sciences, Dalian National Laboratory for Clean Energy, Dalian 116023, China

[‡]Graduate University of Chinese Academy of Sciences, Beijing 100049, China

Supporting Information

ABSTRACT: The oxygen evolution is kinetically the key step in the photocatalytic water splitting. Cocatalysts could lower the activation potential for O_2 evolution. However, the cocatalyst for O_2 evolution has been less investigated, and few effective cocatalysts were reported. This paper reports that the O_2 evolution rate of photocatalytic water splitting under visible light irradiation can be significantly enhanced when the electrocatalyst cobalt–phosphate (denoted as CoPi) was deposited on $BiVO_4$. The photocurrent density is also greatly enhanced by loading CoPi on $BiVO_4$ electrode, and this enhancement in performance shows the similar trend between the photocatalytic activity and photocurrent density. We also found that this tendency is true for $BiVO_4$ loaded with a series of different electrocatalysts as the cocatalysts. These results demonstrate that an effective electrocatalyst of water oxidation can be also an effective cocatalyst for O_2 evolution from photocatalytic water oxidation. By depositing the CoPi as the oxidation cocatalyst and Pt as the reduction cocatalyst on an yttrium-doped $BiVO_4$ ($Bi_{0.5}Y_{0.5}VO_4$), overall water splitting reaction to H_2 and O_2 was realized. Our work also reveals the essential relations between photocatalysis and electrocatalysis in water splitting reaction.

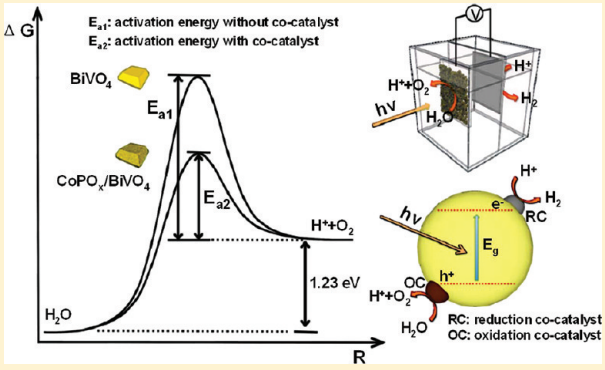

1. INTRODUCTION

Producing renewable clean energy has become one of the most profound challenges of the 21st century.[1−4] Most of the world's current energy supplies come from the chemical energy converted by photosynthesis process from sunlight.[5,6] A central thrust of the current energy research focuses on the artificial photosynthesis.[7,8] In the work on artificial photocatalysts, it has been demonstrated that cocatalysts can enhance the activity of photocatalytic H_2 production.[9−25] The major challenge for water splitting is the O_2 evolution, which is an uphill reaction involved a four-electron transfer process, so the research on the photocatalytic oxygen evolution has recently been intensified as it serves as the key step for the artificial water oxidation. However, only a few noble metal oxides, such as RuO_2 and IrO_2, were found to be good oxidation cocatalysts for photocatalytic O_2 evolution from water oxidation.[26−28] Developing a viable water oxidation cocatalyst to achieve the water oxidation has become particularly crucial for the water splitting reaction.

Similar to photocatalytic water splitting, the electrocatalytic splitting of water involves two concurrent catalytic half-cell reactions: $2H^+ + 2e^- \rightarrow H_2$ and $2H_2O \rightarrow 4H^+ + O_2 + 4e^-$. Clearly, water oxidation being a four-electron process is more complex as compared to the evolution of hydrogen.[29] Recently, Nocera's group reported a robust electrochemical water oxidation catalyst based on earth-abundant cobalt phosphate (CoPi), which possesses attractive features such as the low overpotential, low cost, and self-repair property.[30−34] Photoeletrochemical water oxidation on α-Fe_2O_3,[35−37] ZnO,[38] WO_3,[39] and Si[40] photoanodes was found to be increased when they were combined with CoPi, and CoPi also markedly improves the photoeletrochemical performance of W:$BiVO_4$,[41,42] while our present work was in progress. However, these researches described the phenomena on the enhanced photocurrent in the photoelectrochemical water oxidation, and no report on the enhancement of photocatalytic O_2 activity from photocatalytic water splitting. Also, the relation between photocatalytic activity and the photocurrent was not discussed before. It is highly desirable to investigate whether this highly active CoPi electrocatalyst can be an effective cocatalyst of photocatalyst for the photocatalytic O_2 evolution from the water splitting.

Herein, we report that the photocatalytic activity of O_2 evolution on $BiVO_4$ photocatalyst can be enhanced to about

Received: November 3, 2011
Published: February 1, 2012

6.8 times after depositing the electrocatalyst CoPi as cocatalyst. CoPi/$BiVO_4$ photoelectrode also shows an enhanced photocurrent density up to about 4.3 times of that of bare $BiVO_4$ electrode. We also found the similar relations between the photocurrent density and photocatalytic activity of O_2 evolution are obtained when the oxidation cocatalysts are extended to CoO_x, IrO_x, MnO_x, and RuO_x. The overall water splitting reaction on Pt−CoPi/$Bi_{0.5}Y_{0.5}VO_4$ was achieved by coloading the oxidation cocatalyst, CoPi, and the reduction cocatalyst, Pt. This further demonstrated the important role of cocatalyst, particularly the oxidation cocatalyst, played in water splitting reaction.

2. EXPERIMENTAL SECTION

2.1. Preparation of Photocatalyst and Film Electrode. All chemicals were analytical grade and used as received without further purification. In a typical procedure, NH_4VO_3 (36.0 mmol) and $Bi(NO_3)_3{\cdot}5H_2O$ (36.0 mmol) were dissolved in 220 and 80 mL of 2.0 M nitric acid solutions, respectively. Then the above solutions were mixed to form a stable yellow homogeneous solution. The pH value of the resulting solution was adjusted to ∼2.0 with ammonia solution under constant stirring. An orange precipitate was obtained during the adjustment of the pH value of the solution, and the suspension was further stirred for 0.5 h. After subsiding for 2 h, the slurry of the orange precipitate (about 70 mL) at the bottom of the beaker was transferred to a Teflon-lined stainless steel autoclave with a capacity of 100 mL and hydrothermally treated at 473 K for 24 h. After the autoclave was cooled to room temperature, a vivid yellow powder was obtained. The powder was separated by filtration, washed, and dried.

$BiVO_4$ powder was loaded with CoPi cocatalyst by the in situ photochemical deposition method in potassium phosphate buffer solution (0.1 M) containing the desired amount of $CoCl_2$ (0.5 mM corresponds to 0.44 wt % Co) for 1 h (denoted as "0.44 wt % CoPi/$BiVO_4$").

$BiVO_4$ film electrodes were prepared by electrophoretic deposition on conducting glass supports (fluorine-doped tin oxide (FTO) substrate). The electrophoretic deposition was carried out in an acetone solution (75 mL) containing iodine (20 mg) and $BiVO_4$ powder ground finely (150 mg), which was dispersed by sonication for 3 min. The FTO electrodes (1.1 × 2 cm) was immersed, parallel with the Pt electrode, in the solution with ca. 8 cm of distance, and then 20 V of bias was applied between them for 1 min using a potentiostat (ITECH IT6834). After this process was repeated four times, the electrode was dried and then calcined at 673 K for 30 min. The $BiVO_4$-coated area was controlled to be ca. 1.1 × 1.5 cm. This procedure resulted in formation of $BiVO_4$ layer having relatively uniform thickness of ca. 2 μm, with good reproducibility. The average weight of $BiVO_4$ deposited on FTO was 1 mg. $BiVO_4$ electrodes were loaded with CoPi cocatalyst by the in situ photochemical deposition method, carried out in a Pyrex reactor in 0.1 M pH 7.0 potassium phosphate solutions containing 0.5 mM $CoCl_2$, and illuminated from the top using a 300 W Xe lamp. CoPi/$BiVO_4$ electrodes with different loadings of CoPi cocatalyst were carefully prepared by controlling the photodeposition time (denoted as CoPi/$BiVO_4$-x).[38] Cocatalysts MO_x (M: Co, Ir, Mn, and Ru) were deposited on the surface of $BiVO_4$ photocatalyst and electrode as a cocatalyst for water oxidation by the impregnation method. The precursor of metal was prepared with the same concentration of the solution (0.187 mg/mL $Co(NO_3)_2$, H_2IrCl_6, $Mn(NO_3)_2$, and $RuCl_3$). After dipping the electrode in the precursor solution, it was quickly taken out and dried at 353 K for 10 min. Then the process was repeated again. Finally, the electrode was calcined at 623 K for 1 h.

$Bi_{0.5}Y_{0.5}VO_4$ powders were prepared by conventional solid-state reactions. Starting materials of Bi_2O_3, Y_2O_3, and V_2O_5 were mixed in a stoichiometric ratio in the presence of suitable ethanol to mix them fully with the ball mill for 4 h. The mixture was calcined at 1073 K for 12 h in the muffle furnace using corundum crucibles. After cooling to the room temperature, the powder was finely ground and calcined at 1123 K for 14 h. The cocatalysts (Pt and CoPi) were loaded over the obtained photocatalysts by a photodeposition method from H_2PtCl_6 and $CoCl_2$ precursors, respectively.

2.2. Characterization of Catalysts. The prepared samples were characterized by X-ray powder diffraction (XRD) on a Rigaku D/Max-2500/PC powder diffractometer. Each sample powder was scanned using Cu Kα radiation with an operating voltage of 40 kV and an operating current of 200 mA. The scan rate of 5°/min was applied to record the patterns in the range of 8−80° at a step size of 0.02°. UV−vis (UV−vis) diffuse reflectance spectra were recorded on a UV−vis spectrophotometer (JASCO V-550) equipped with an integrating sphere. X-ray photoelectron spectroscopy (XPS) measurements were performed using a VG ESCALAB MK2 spectrometer with monochromatized Al Kα excitation. The morphologies and particle sizes were examined by scanning electron microscopy (SEM) taken with a Quanta 200 FEG scanning electron microscope.

2.3. Photocatalytic Reactions and Photocurrent Measurements. The photocatalytic O_2 evolution reactions were carried out in a closed gas circulation and evacuation system. Typically, 0.2 g of catalyst was dispersed by a magnetic stirrer in 0.1 M pH 7.0 potassium phosphate buffer solution containing 0.8 g of $NaIO_3$ (0.02 M, 200 mL) in a reaction cell made of Pyrex glass. The suspension was then thoroughly degassed and irradiated by an ozone-free 300 W Xe lamp (CERMAX, LX300) from the top of the reaction cell. A cutoff filter (Kenko, L-42; λ > 420 nm) was equipped to eliminate ultraviolet light. A Pyrex glass water filter, filled with water, was placed between the Xe lamp and the reaction cell to remove the infrared light. The temperature of the reactant solution was maintained at 15 ± 2 °C with cooling water during the reaction. The amount of evolved O_2 was analyzed by an online gas chromatograph (Shimadzu GC-8A, TCD, Ar carrier). Photocatalytic reactions of $Bi_{0.5}Y_{0.5}VO_4$ catalyst for overall water splitting were carried out in a gas-closed circulation system a 300 W Xe illuminator (CERMAX; LX300). 0.2 g of catalyst was dispersed in 200 mL of pure water in a Pyrex reactor. The suspension was then thoroughly degassed and irradiated by an ozone-free 300 W Xe lamp (CERMAX, LX300) from the top of the reaction cell. The temperature of the reactant solution was maintained at 15 ± 2 °C with cooling water during the reaction. The amounts of H_2 and O_2 evolved were determined using gas chromatography (Shimadzu; GC-8A, TCD, Ar carrier).

Before the photocurrent measurements, the areas of all the electrodes was fixed to 0.36 cm^2 by the insulating cement. (see Supporting Information Figure S1). Photoelectrochemical performance of $BiVO_4$ electrode was measured in a three-electrode setup in a 0.1 M potassium phosphate solution (pH 7.0). The counter electrode was platinum electrode, and the reference electrode was saturation mercury electrode (SCE) in 0.1 M potassium phosphate buffer solution (pH = 7).

dx.doi.org/10.1021/jp210584b | J. Phys. Chem. C 2012, 116, 5082−5089

For linear sweep voltammetry, potential was swept to the negative direction with a scan rate of 10 mV/s. A shutter was used to record both the dark and photocurrent during a single scan.

3. RESULTS AND DISCUSSION

3.1. Characterizations of $BiVO_4$ and CoPi/$BiVO_4$ Photocatalyst and Photoelectrode. Figure 1a shows the

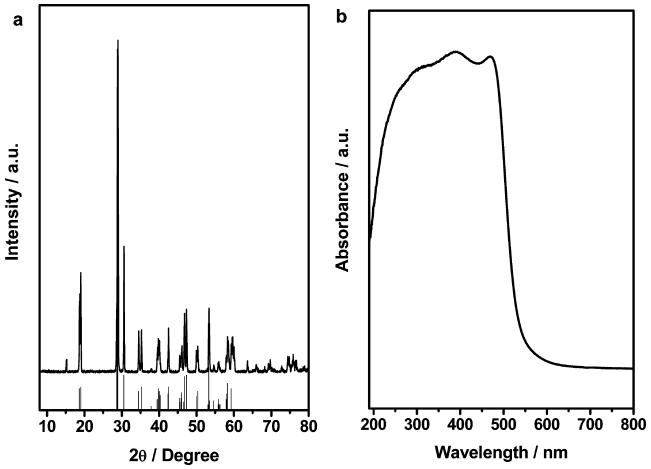

Figure 1. (a) XRD of $BiVO_4$ synthesized by the hydrothermal method. (b) UV−vis diffuse reflectance spectra of $BiVO_4$ synthesized by the hydrothermal method.

XRD pattern of $BiVO_4$ synthesized by hydrothermal treatment at 200 °C for 24 h. The XRD pattern of $BiVO_4$ was assigned to monoclinic scheelite $BiVO_4$ which is in good agreement with the standard card of No. 14-0688 (space group: $I2/a$, a = 5.195, b = 11.701, c = 5.092, β = 90.38). Characteristic diffraction peaks located at 15.1°, 18.6°, 18.9°, 28.6°, 28.8°, 28.9°, and 30.5° are all ascribed to the monoclinic scheelite $BiVO_4$. The UV−vis diffuse reflectance spectrum of $BiVO_4$ powder prepared hydrothermally is shown in Figure 1b. $BiVO_4$ shows strong absorption in the visible light region until 535 nm. The steep shape of the spectrum indicates that the visible light adsorption is not due to the transition from the impurity level but to the bandgap transition. The energy of the band gap of $BiVO_4$ estimated from the main absorption edge of the UV−vis diffuse reflectance spectrum is 2.31 eV.

SEM images clearly show smooth surface, quite regular decahedron shape and excellent crystallinity of $BiVO_4$ (Figure 2). At low magnification, large compact particles with decagonal shape were observed for $BiVO_4$ sample (Figure 2a). There was a negligible quantity of small irregular particles adhering to the decagonal particles. The formation of domains with smooth surfaces was observed. These domains ended with well-defined walls, the edges of which were relatively very sharp. Figure 2c shows the SEM images of CoPi/$BiVO_4$ catalyst synthesized by the photochemically deposited method. After the photochemical deposition of CoPi cocatalyst on $BiVO_4$, the cocatalyst was deposited as nanoparticles on the $BiVO_4$ surface with high dispersion. The photochemically deposition allows the cocatalysts to be loaded at the reaction sites, unnecessary for a further activation treatment.[43]

XPS was used to examine the surface composition of Co, P, and O in the CoPi/$BiVO_4$ samples. Figure S3 shows the Co 2p and P 2p spectra of CoPi/$BiVO_4$ before and after smoothing, respectively. The XPS study showed that the cobalt 2p of the photochemically deposited photocatalysts was determined by the peaks at 780 and 795.5 eV, suggesting that they are composed of the Co catalytic centers (Figure 3a,b). The phosphorus 2p XPS of the photochemically deposited CoPi

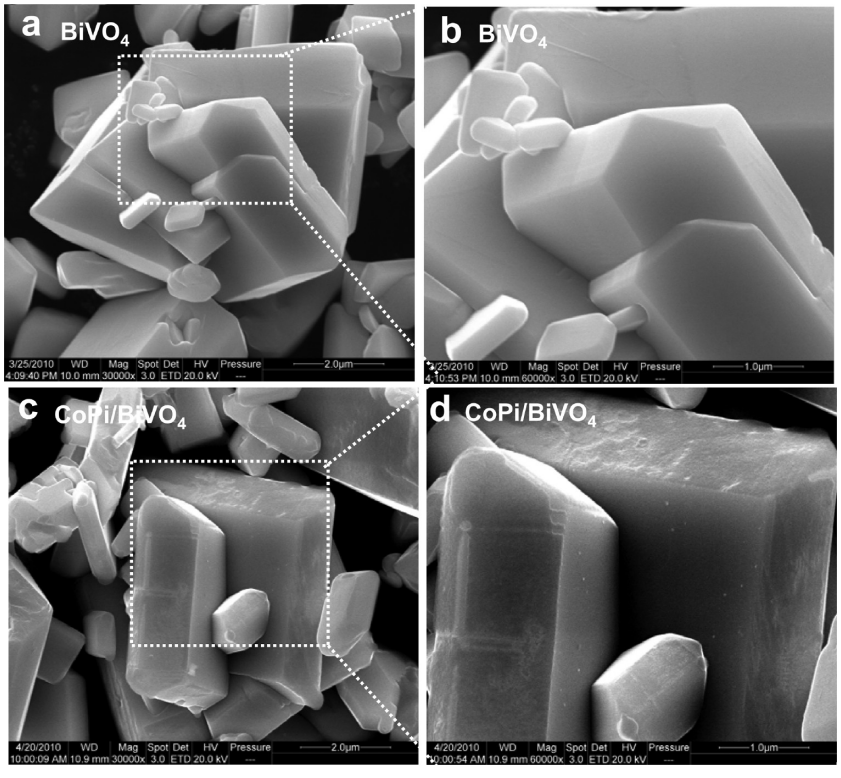

Figure 2. SEM images of (a) $BiVO_4$, (b) $BiVO_4$ at high resolution, (c) CoPi/$BiVO_4$, and (d) CoPi/$BiVO_4$ at high resolution.

dx.doi.org/10.1021/jp210584b | J. Phys. Chem. C 2012, 116, 5082−5089

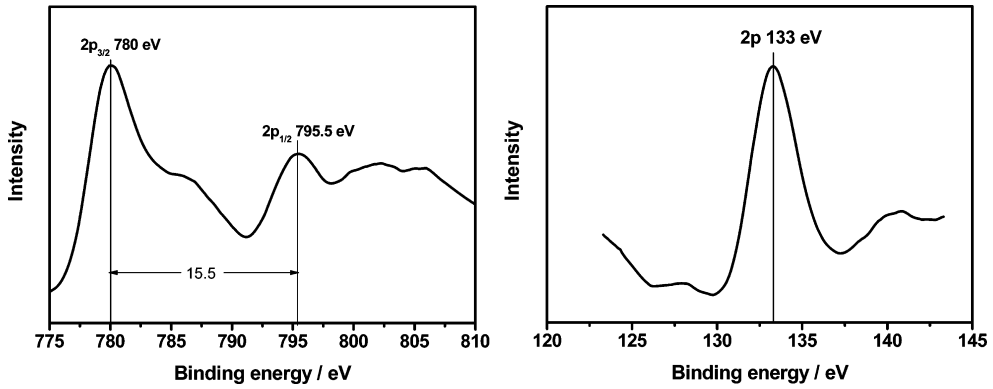

Figure 3. XPS spectra of the CoPi/$BiVO_4$: (a) the Co 2p and (b) P 2p peaks.

cocatalyst show a peak at 133 eV due to the phosphate contained in the photocatalyst (Figure 3c,d)

Figure 4 shows SEM images of $BiVO_4$ electrodes without and with CoPi cocatalyst. To prepare compact $BiVO_4$ film electrode, the powder was ground finely. $BiVO_4$ particles were deposited on FTO conducting glass by the electrophoretic deposition method. The surfaces of both the electrodes were essentially flat without any crack (Figure 4a,c). At higher resolution, the FTO substrate surface could not be observed, as shown in Figure 4b,d. Before coating the powder onto the FTO conduct glass, the powder was ground finely, so there are plenty broken small particles in Figure 4d. However, the large decagonal particles still demonstrate smooth surface and well domain. Compared with the smooth surface of the $BiVO_4$ electrode without CoPi cocatalyst, there are apparent nanoparticles on the CoPi/$BiVO_4$ electrode, which are distributed uniformly in Figure 4c,d. Energy dispersive spectroscopy (EDS) shows that the ratio of P/Co in photochemically deposited CoPi on $BiVO_4$ electrode is about 0.90 for the $BiVO_4$ photocatalyst (Figure 4e). This P/Co ratio is lower than that of the accurate value because the Bi peak and P peak overlapping affects the fraction of surface P atoms in the photocatalyst. For the $BiVO_4$ electrode, the ratio of P/Co is about 0.90, which is lower than the accurate value also. Therefore, we can conclude that the EDS results prove that the CoPi cocatalyst can be successfully loaded on the $BiVO_4$ electrode by the photochemically deposited method.

3.2. Photocatalytic O_2 Evolution and Photocurrent Density of CoPi/$BiVO_4$ and MO_x/$BiVO_4$. Figure 5a shows the O_2 evolution on CoPi/$BiVO_4$ catalysts with different CoPi loadings, together with that on $BiVO_4$ for a comparison. After loading CoPi on $BiVO_4$, the photocatalytic activity of O_2 evolution on CoPi/$BiVO_4$ is increased to a maximum when the loading of CoPi is about 1.0 wt %. The activity is increased by up to 6.8 times, compared with that for $BiVO_4$. This unambiguously indicates that the electrocatalyst CoPi can act as an efficient cocatalyst of photocatalyst for O_2 evolution from water oxidation.

Figure 5b shows the photocurrent density measured at a constant bias of 0.3 V against the SCE reference electrode for $BiVO_4$ electrode. For the $BiVO_4$ electrode, the photocurrent density is relatively very low. Photochemically depositing CoPi on bare $BiVO_4$ electrode for 10 min resulted in an obvious improvement in the photocurrent density. Increasing the deposited time to 20 min afforded a further increase in photocurrent density to a maximum for the CoPi/$BiVO_4$-20 electrode by 4.3 times that of bare $BiVO_4$ electrode (Figure 5b). It is estimated that the loading of CoPi on $BiVO_4$ is approximately linearly increased with the deposition time. From Figure 2, we can found that the photocatalytic activity of O_2 evolution and the photocurrent density are enhanced to a maximum and show same trend with increasing the loading of CoPi.

This correlation between the activity of O_2 evolution and photocurrent density for CoPi/$BiVO_4$ is found to be also true for MO_x/$BiVO_4$ catalysts with a series of different kinds of cocatalysts (MO_x: CoO_x, IrO_x, MnO_x, RuO_x) (Figure 6). As typical oxidation cocatalysts, ruthenium oxide, iridium oxide, cobalt oxide, and manganese oxide have been found to be active electrocatalysts for electrocatalytic water oxidation.[44−48] 0.44 wt % of these cocatalysts was loaded on $BiVO_4$ with the impregnation method from the corresponding metal complexes. Among the cocatalyst tested, CoPi is demonstrated to be the most efficient cocatalyst for O_2 evolution, while the rate of O_2 evolution of CoO_x/$BiVO_4$ is slightly lower than that of CoPi/$BiVO_4$, suggesting that CoO_x exhibits similar cocatalyst property to CoPi (Figure 6a). Figure 6b shows the photocurrent densities measured at a constant bias of 0.5 V against the SCE reference electrode for MO_x/$BiVO_4$ electrodes. It is noteworthy that the two curves shown in Figure 6a,b are very analogous to each other. Correspondingly, the CoPi/$BiVO_4$ elecrode demonstrates the highest photocurrent density. This suggests that the performance of electrocatalysts is in parallel with that of cocatalysts of photocatalyst for water splitting reaction. Accordingly, the electrocatalyst with high activity in electrolysis of water shows the high activity as a cocatalyst in photocatalysis for water oxidation reaction.

Figure 7a shows that all photoelectrodes generated anodic photocurrent densities upon illumination due to the ability of $BiVO_4$ for water oxidation. The onset potential of CoPi/$BiVO_4$-20 electrode was observed at approximately −0.05 V vs SCE, which corresponds to 0.3 V vs SCE for bare $BiVO_4$ electrode. That is, the onset potential of the CoPi/$BiVO_4$-20 electrode is shifted to the negative direction by 0.35 V compared to that of the $BiVO_4$ electrode. The observed shift of the photocurrent onset potential can be attributed to the presence of CoPi cocatalyst. The effect of CoPi cocatalyst is also evident in the general enhancement of anodic photocurrent density observed in the entire potential range shown in Figure 7a. However, the photocurrent density enhancement by CoPi cocatalyst becomes less significant for CoPi/$BiVO_4$ with higher loading of CoPi. The effect of cocatalysts is also evident on the anodic photocurrent observed in the entire potential range shown in Figure 7b. The effect of the MO_x cocatalysts on photocurrent generation of $BiVO_4$ electrode was investigated by comparing photocurrent−potential characteristics of $BiVO_4$ electrodes

dx.doi.org/10.1021/jp210584b | J. Phys. Chem. C 2012, 116, 5082−5089

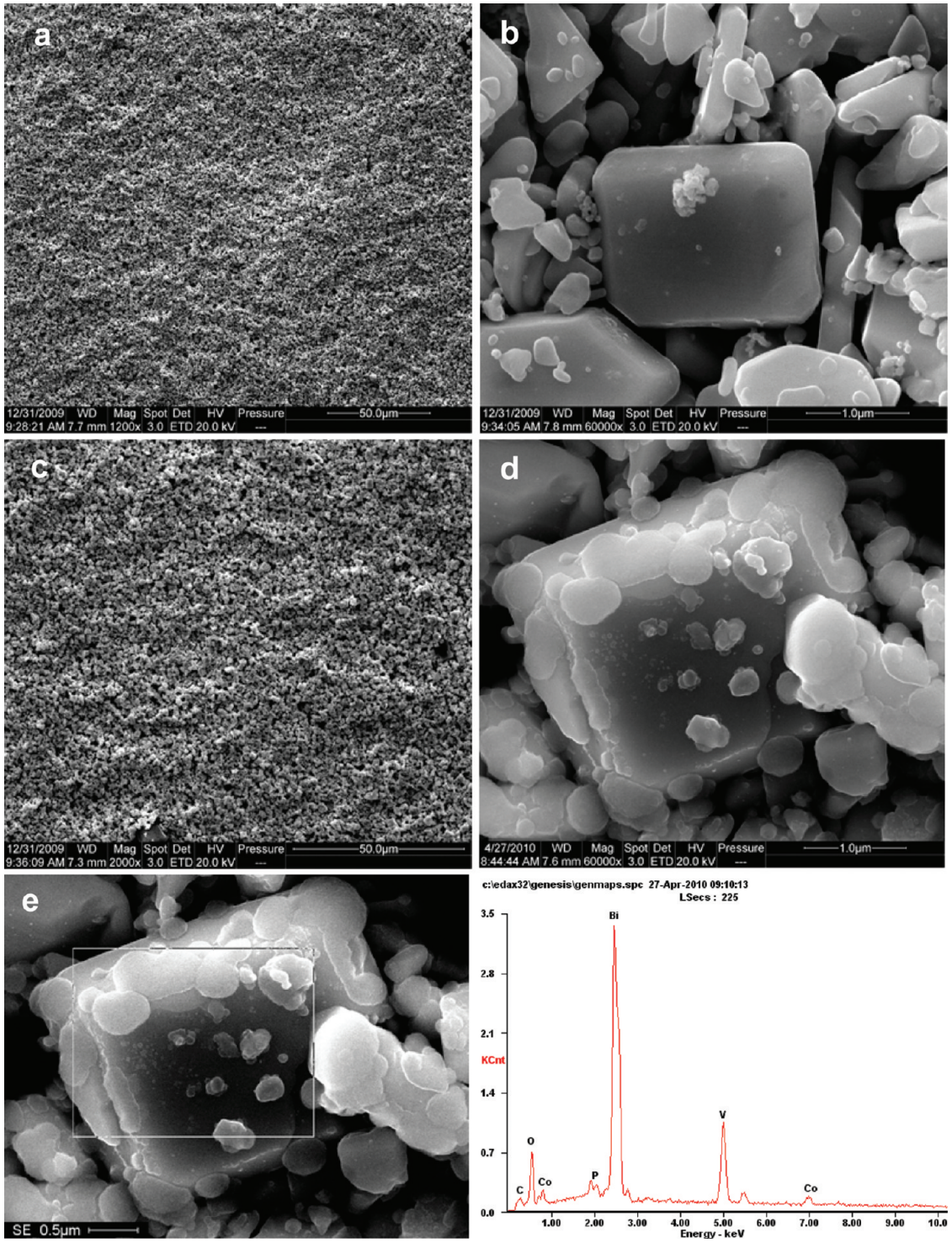

Figure 4. SEM images of $BiVO_4$ electrodes (a, b) without and (c, d) with CoPi cocatalyst. (e) EDS data of CoPi/$BiVO_4$ electrode.

with MO_x cocatalyst (Figure 7b). Figure 7b shows that all electrodes generated anodic photocurrent densities upon illumination due to the ability of $BiVO_4$ for water oxidation. The onset potential of $BiVO_4$ electrode was observed at approximately 0.3 V vs SCE, while the onset potential of $CoO_x/BiVO_4$ electrode was ca. 0.1 V vs SCE. However, for $IrO_x/BiVO_4$, $MnO_x/BiVO_4$, and $RuO_x/BiVO_4$ electrodes, the onset potentials were 0.2, 0.35, and 0.4 V, respectively. The onset potentials of the $CoO_x/BiVO_4$ and $IrO_x/BiVO_4$ electrodes are shifted to the negative direction by 0.2 and 0.1 V compared to that of bare $BiVO_4$ electrode.

3.3. Essential Relations between Electrocatalyst and Photocatalyst. The activity of water oxidation is correlated with the photocurrent density of the photoelectrode.

Based on the law of the energy conservation

$$\text{photocatalysis:} \quad E_g \geq E^{\ominus} + E_a \tag{1}$$

dx.doi.org/10.1021/jp210584b | J. Phys. Chem. C 2012, 116, 5082–5089

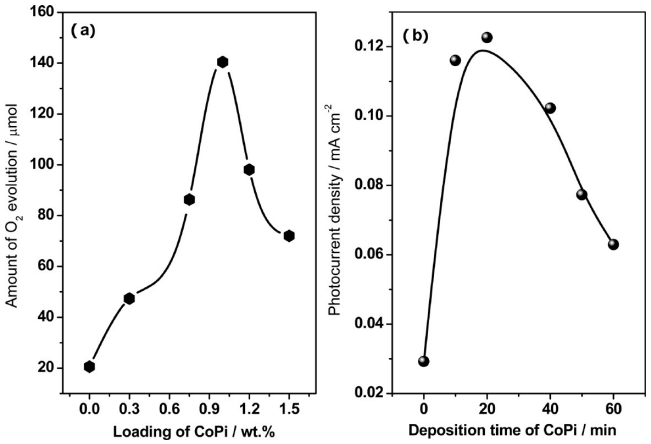

Figure 5. (a) Photocatalytic O_2 evolution on CoPi/$BiVO_4$ with different loadings of CoPi. Reaction conditions: 0.2 g of catalyst; 0.1 M pH 7.0 potassium phosphate buffer solution containing 0.8 g of $NaIO_3$ solution (200 mL); reaction time, 3 h; light source, Xe lamp (300 W) with a cutoff filter ($\lambda \geq 420$ nm). (b) Photocurrent densities of CoPi/$BiVO_4$ electrodes with different deposited times measured at 0.3 V against the SCE reference electrode. Electrolyte: 0.1 M pH 7.0 potassium phosphate buffer solution.

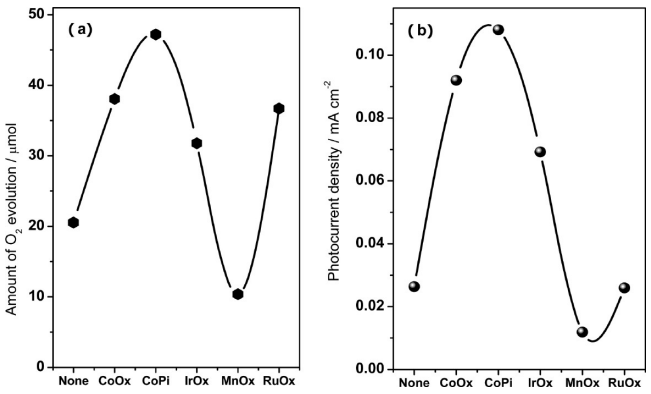

Figure 6. (a) Photocatalytic O_2 evolution on 0.44 wt % MO_x/$BiVO_4$ prepared by the impregnation method. Reaction conditions: 0.2 g of catalyst; 0.1 M pH 7.0 potassium phosphate buffer solution containing 0.8 g of $NaIO_3$ (200 mL); reaction time, 3 h; light source, Xe lamp (300 W) with a cutoff filter ($\lambda \geq 420$ nm). (b) Photocurrent densities of MO_x/$BiVO_4$ electrodes with the same loading of MO_x measured at 0.5 V against the SCE reference electrode. Electrolyte: 0.1 M pH 7.0 potassium phosphate buffer solution.

$$\text{photoelectrocatalysis:} \quad E_g + E_V \geq E^{\ominus} + E_{AOP} \tag{2}$$

$$\text{Arrhenius equation:} \quad k = A \exp(-E_{AOP}/RT) \tag{3}$$

where $E^{\ominus}$ is chemical energy at the standard potential for O_2 evolution (1.23 V), E_a is the activation energy, and E_{AOP} is the activation energy in photocatalytic and photoelectrocatalytic water oxidation; the activation overpotential is denoted as AOP; E_g is the band gap (2.30 eV) of $BiVO_4$; E_V is the externally applied electric energy at the onset potential.

For the water splitting reaction, the activation energy for the reduction reaction for H_2 production is very low, so here we mainly discuss the activation energy of the water oxidation. After loading CoPi as cocatalyst, the negative shift of photocurrent onset potential for CoPi/$BiVO_4$ electrode, ca. 0.35 V, suggests that less external electric energy, ca. 0.35 eV, is applied during the photoelectrochemical water oxidation (Figure 7a). That is, CoPi loaded on $BiVO_4$ electrode can lead to lower E_{AOP} for water oxidation for both photocatalytic and photoelectrochemical water oxidation. Besides, when different electrocatalysts were loaded on $BiVO_4$ as cocatalysts, the photocatalytic O_2 evolution and the photocurrent density follow the same order: CoPi/$BiVO_4$ > CoO_x/$BiVO_4$ > IrO_x/$BiVO_4$ > $BiVO_4$ > MnO_x/$BiVO_4$, except RuO_x/$BiVO_4$ (Figure 7). However, the E_V is increased as the photocatalytic activity and photocurrent density is decreased (Figure 7b). Therefore, according to eq 2, the E_{AOP} should be in the contrary order of CoPi/$BiVO_4$ < CoO_x/$BiVO_4$ < IrO_x/$BiVO_4$ < $BiVO_4$ < MnO_x/$BiVO_4$ < RuO_x/$BiVO_4$. RuO_2 is found to be good oxidation cocatalysts for O_2 evolution, but RuO_2 is also found to be a reduction cocatalyst.[26] That may be the reason why RuO_x is an exception in this system. Cocatalysts offer the low E_{AOP} for photocatalytic water oxidation and are often served as the active sites for the O_2 generation. So decreasing the activation overpotential is crucial for promoting the photocatalytic water oxidation by employing suitable cocatalyst to lower the activation overpotential.

The fact that loading CoPi on $BiVO_4$ as cocatalyst, both the photocatalytic activity of O_2 evolution and the photocurrent density are significantly enhanced (Figure 5), leads us to the conclusion that the loaded cocatalyst decreases the activation energy, E_a, of photocatalytic water oxidation as that the electrocatalyst reduces the overpotential of water electrocatalysis. The activation overpotential (denoted as AOP) is essentially related with the activation energy (eq 2). CoPi is an effective electrocatalyst which reduces the overpotential to 0.41 V.[30] CoPi as cocatalyst correspondingly could reduce the activation energy, resulting in the high activity in photocatalytic water oxidation. Besides, for $BiVO_4$ electrode, the loaded CoPi - on $BiVO_4$ can decrease the recombination of hole/electron at the near flat band potential due to the negative shift of the onset potential. In the photoelectrochemical studies, the loaded CoPi may involve a multistep of the valency change that is preceded by a hole stream from $BiVO_4$ to the active site, CoPi.[42] The phosphate electrolyte plays the essential role of maintaining this charge equilibrium by facilitating rapid hole trap in both photocatalytic reaction and photoelectrochemical processes.

3.4. Overall Water Splitting on $Bi_{0.5}Y_{0.5}VO_4$ with Cocatalyst. $BiVO_4$ was reported to show high activity of O_2 evolution with sacrificial reagent but not able to evolve H_2 because its conduction band is not negative enough.[49−51] Figure 8a shows the XRD patterns for $Bi_{0.5}Y_{0.5}VO_4$ sample obtained by calcining the mixture of Bi_2O_3, Y_2O_3, and V_2O_5 at 1073 K for 12 h. The standard cards of $BiVO_4$ (No. 14-0133) and YVO_4 (No. 72-0861) data are shown for comparison. The positions of the diffraction peaks were successively shifted to the position between pure $BiVO_4$ and YVO_4, indicating that the obtained samples were not physical mixtures of $BiVO_4$ and YVO_4 but rather solid solutions of $BiVO_4$ and YVO_4. Figure 8b shows the UV−vis diffuse reflectance spectra for $Bi_{0.5}Y_{0.5}VO_4$. The absorption edge of $Bi_{0.5}Y_{0.5}VO_4$ is estimated to be 500 nm.

To further demonstrate the role of CoPi in the photocatalytic water oxidation, CoPi was loaded on a yttrium-doped $BiVO_4$, $Bi_{0.5}Y_{0.5}VO_4$ (denoted as BYVO), which is a semiconductor being thermodynamically able to achieve overall water splitting, but its activity without loading cocatalysts is very low (Figure 9). After loading 0.1 wt % Pt on BYVO, H_2 production is obviously increased, indicating that Pt is the reduction cocatalyst

dx.doi.org/10.1021/jp210584b | J. Phys. Chem. C 2012, 116, 5082−5089

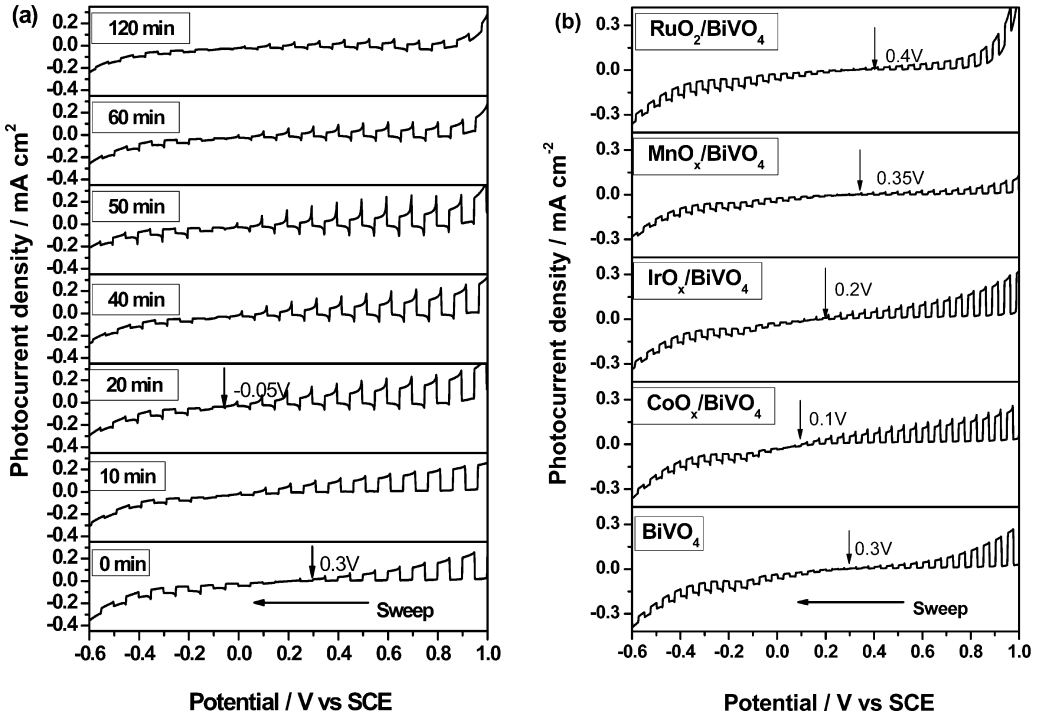

Figure 7. Photocurrent measurement. (a) Photocurrent−potential characteristics of $BiVO_4$ and CoPi/$BiVO_4$ electrodes with different deposited times of CoPi measured (scan rate, 10 mV/s) with chopped light. (b) Photocurrent−potential characteristics of $BiVO_4$ and MO_x/$BiVO_4$ electrodes with the same loading of MO_x measured (scan rate, 10 mV/s) with chopped light. Electrolyte: 0.1 M pH 7.0 potassium phosphate buffer solution.

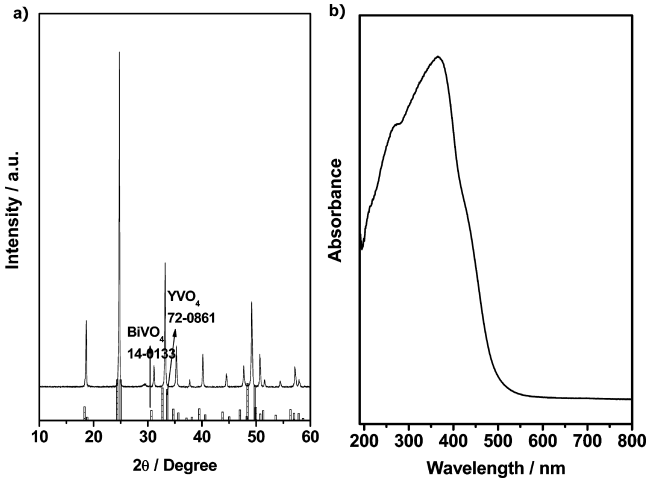

Figure 8. (a) XRD of $Bi_{0.5}Y_{0.5}VO_4$ synthesized by solid state reaction. (b) UV−vis diffuse reflectance spectra of $Bi_{0.5}Y_{0.5}VO_4$ synthesized by solid state reaction.

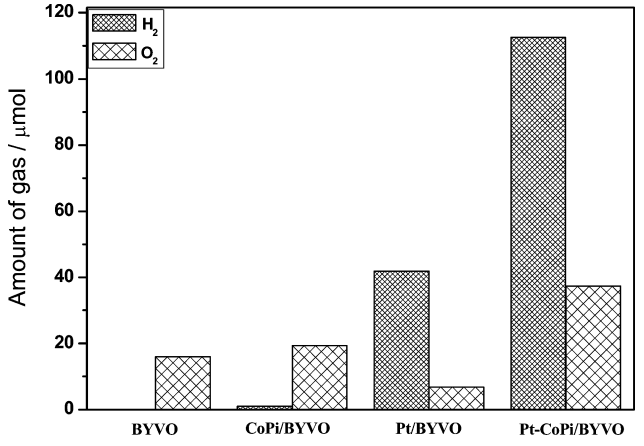

Figure 9. Photocatalytic water splitting on $Bi_{0.5}Y_{0.5}VO_4$ loaded with CoPi and Pt from pure water. Reaction conditions: 0.2 g of catalyst; pure water (200 mL); light source, Xe lamp (300 W), reaction time, 9 h.

promoting H_2 evolution, but the activity for overall water splitting is still low. When 0.1 wt % CoPi was loaded on BYVO, the activities of H_2 and O_2 evolution are still low, suggesting CoPi does not act as a reduction cocatalyst. Co-loading the electrocatalyst 0.1 wt % CoPi and reduction cocatalyst Pt on BYVO, both the activities of H_2 and O_2 evolutions can be enhanced to almost 3 times of that for 0.1 wt % Pt/BYVO. From the results,it can be deduced that the CoPi mainly contributes to the O_2 evolution. Accordingly, dual cocatalysts enhance the activity of overall water splitting on 0.1 wt % Pt−0.1 wt % CoPi/BYVO.

4. CONCLUSION

We demonstrated that the active electrocatalyst CoPi as a cocatalyst on $BiVO_4$ can be also an active cocatalyst for photocatalytic water oxidation. We also found the similar trend and revealed the essential relations between the photocatalytic activity of O_2 evolution and the photocurrent density of CoPi/$BiVO_4$ photoelectrode, as the oxidation of water is the key step in the water splitting reaction. The enhancement of photocatalytic activity and photocurrent density can be attributed to the cocatalyst and electrocatalyst which lower the activation energy and overpotential for water oxidation of photocatalysis and electrocatalysis, respectively. By taking the advantages of

dx.doi.org/10.1021/jp210584b | J. Phys. Chem. C 2012, 116, 5082−5089

cocatalysts, the overall water splitting reaction was achieved on Pt-CoPi/$Bi_{0.5}Y_{0.5}VO_4$.

■ ASSOCIATED CONTENT

Supporting Information

Pictures of $BiVO_4$ electrodes. This material is available free of charge via the Internet at http://pubs.acs.org.

■ AUTHOR INFORMATION

Corresponding Author

*E-mail: canli@dicp.ac.cn; Tel: 86-411-84379070; Fax: 86-411-84694447.

■ ACKNOWLEDGMENTS

This work was financially supported by National Program on Key Basic Research Project (Grant 2009CB220010), National Natural Science Foundation of China (Grant 21061140361), and Solar Energy Action Plan of Chinese Academy of Sciences (Grant KGCX2-YW-393-1).

■ REFERENCES

(1) Chow, J.; Kopp, R. J.; Portney, P. R. *Science* **2003**, *302*, 1528.
(2) Chen, X.; Shen, S.; Guo, L.; Mao, S. S. *Chem. Rev.* **2010**, *110*, 6503.
(3) Chen, X.; Liu, L.; Yu, P. Y.; Mao, S. S. *Science* **2011**, *331*, 746.
(4) Walter, M. G.; Warren, E. L.; McKone, J. R.; Boettcher, S. W.; Mi, Q.; Santori, E. A.; Lewis, N. S. *Chem. Rev.* **2010**, *110*, 6446.
(5) Takanabe, K.; Uzawa, T.; Wang, X. C.; Maeda, K.; Katayama, M.; Kubota, J.; Kudo, A.; Domen, K. *Dalton Trans.* **2009**, 10055.
(6) Kudo, A.; Miseki, Y. *Chem. Soc. Rev.* **2009**, *38*, 253.
(7) Lewis, N. S.; Nocera, D. G. *Proc. Natl. Acad. Sci. U. S. A.* **2006**, *103*, 15729.
(8) Balzani, V.; Credi, A.; Venturi, M. *ChemSusChem* **2008**, *1*, 26.
(9) Linsebigler, A. L.; Lu, G. Q.; Yates, J. T. *Chem. Rev.* **1995**, *95*, 735.
(10) Yan, H.; Yang, J.; Ma, G.; Wu, G.; Zong, X.; Lei, Z.; Shi, J.; Li, C. *J. Catal.* **2009**, *266*, 165.
(11) Zong, X.; Yan, H. J.; Wu, G. P.; Ma, G. J.; Wen, F. Y.; Wang, L.; Li, C. *J. Am. Chem. Soc.* **2008**, *130*, 7176.
(12) Trasatti, S. *J. Electroanal. Chem.* **1972**, *39*, 163.
(13) Sato, S.; White, J. M. *Chem. Phys. Lett.* **1980**, *72*, 83.
(14) Kitano, M.; Takeuchi, M.; Matsuoka, M.; Thomas, J. M.; Anpo, M. *Catal. Today* **2007**, *120*, 133.
(15) Liu, M. Y.; You, W. S.; Lei, Z. B.; Zhou, G. H.; Yang, J. J.; Wu, G. P.; Ma, G. J.; Luan, G. Y.; Takata, T.; Hara, M.; Domen, K.; Can, L. *Chem. Commun.* **2004**, 2192.
(16) Zhang, F. X.; Maeda, K.; Takata, T.; Domen, K. *Chem. Commun.* **2010**, *46*, 7313.
(17) Maeda, K.; Teramura, K.; Lu, D. L.; Takata, T.; Saito, N.; Inoue, Y.; Domen, K. *J. Phys. Chem. B* **2006**, *110*, 13753.
(18) Maeda, K.; Xiong, A. K.; Yoshinaga, T.; Ikeda, T.; Sakamoto, N.; Hisatomi, T.; Takashima, M.; Lu, D. L.; Kanehara, M.; Setoyama, T.; Teranishi, T.; Domen, K. *Angew. Chem. Int. Ed.* **2010**, *49*, 4096.
(19) Maeda, K.; Teramura, K.; Saito, N.; Inoue, Y.; Domen, K. *J. Catal.* **2006**, *243*, 303.
(20) Maeda, K.; Teramura, K.; Domen, K. *Catal. Surv. Asia* **2007**, *11*, 145.
(21) Maeda, K.; Teramura, K.; Lu, D. L.; Takata, T.; Saito, N.; Inoue, Y.; Domen, K. *Nature* **2006**, *440*, 295.
(22) Kato, H.; Kudo, A. *J. Phys. Chem. B* **2001**, *105*, 4285.
(23) Kato, H.; Asakura, K.; Kudo, A. *J. Am. Chem. Soc.* **2003**, *125*, 3082.
(24) Ikarashi, K.; Sato, J.; Kobayashi, H.; Saito, N.; Nishiyama, H.; Inoue, Y. *J. Phys. Chem. B* **2002**, *106*, 9048.
(25) Ma, B. J.; Wen, F. Y.; Jiang, H. F.; Yang, J. H.; Ying, P. L.; Li, C. *Catal. Lett.* **2010**, *134*, 78.
(26) Sakata, T.; Hashimoto, K.; Kawai, T. *J. Phys. Chem.* **1984**, *88*, 5214.
(27) Iwase, A.; Kato, H.; Kudo, A. *Chem. Lett.* **2005**, *34*, 946.
(28) Ma, B. J.; Yang, J. H.; Han, H. X.; Wang, J. T.; Zhang, X. H.; Li, C. *J. Phys. Chem. C* **2010**, *114*, 12818.
(29) Dau, H.; Limberg, C.; Reier, T.; Risch, M.; Roggan, S.; Strasser, P. *ChemCatChem* **2010**, *2*, 724.
(30) Kanan, M. W.; Nocera, D. G. *Science* **2008**, *321*, 1072.
(31) Kanan, M. W.; Surendranath, Y.; Nocera, D. G. *Chem. Soc. Rev.* **2009**, *38*, 109.
(32) Surendranath, Y.; Dinca, M.; Nocera, D. G. *J. Am. Chem. Soc.* **2009**, *131*, 2615.
(33) Lutterman, D. A.; Surendranath, Y.; Nocera, D. G. *J. Am. Chem. Soc.* **2009**, *131*, 3838.
(34) Esswein, A. J.; Surendranath, Y.; Reece, S. Y.; Nocera, D. G. *Energy Environ. Sci.* **2011**, *4*, 499.
(35) Zhong, D. K.; Sun, J. W.; Inumaru, H.; Gamelin, D. R. *J. Am. Chem. Soc.* **2009**, *131*, 6086.
(36) Zhong, D. K.; Gamelin, D. R. *J. Am. Chem. Soc.* **2010**, *132*, 4202.
(37) Barroso, M.; Cowan, A. J.; Pendlebury, S. R.; Grätzel, M.; Klug, D. R.; Durrant, J. R. *J. Am. Chem. Soc.* **2011**, *133*, 14868.
(38) Steinmiller, E. M. P.; Choi, K. S. *Proc. Natl. Acad. Sci. U. S. A.* **2009**, *106*, 20633.
(39) Seabold, J. A.; Choi, K.-S. *Chem. Mater.* **2011**, *23*, 1105.
(40) Young, E. R.; Costi, R.; Paydavosi, S.; Nocera, D. G.; Bulovic, V. *Energy Environ. Sci.* **2011**, *4*, 2058.
(41) Ye, H.; Park, H. S.; Bard, A. J. *J. Phys. Chem. C* **2011**, *115*, 12464.
(42) Zhong, D. K.; Choi, S.; Gamelin, D. R. *J. Am. Chem. Soc.* **2011**, DOI: 10.1021/ja207348x.
(43) Kraeutler, B.; Bard, A. J. *J. Am. Chem. Soc.* **1978**, *100*, 4317.
(44) Trasatti, S. *J. Electroanal. Chem.* **1980**, *111*, 125.
(45) Burke, L. D.; Murphy, O. J.; Oneill, J. F.; Venkatesan, S. *J. Chem. Soc., Faraday Trans.* **1977**, *73*, 1659.
(46) Shub, D. M.; Chemodanov, A. N.; Shalaginov, V. V. *Sov. Electrochem.* **1978**, *14*, 507.
(47) Iwakura, C.; Tada, H.; Tamura, H. *Denki Kagaku* **1977**, *45*, 202.
(48) Morita, M.; Iwakura, C.; Tamura, H. *Electrochim. Acta* **1979**, *24*, 357.
(49) Sayama, K.; Nomura, A.; Arai, T.; Sugita, T.; Abe, R.; Yanagida, M.; Oi, T.; Iwasaki, Y.; Abe, Y.; Sugihara, H. *J. Phys. Chem. B* **2006**, *110*, 11352.
(50) Kudo, A.; Omori, K.; Kato, H. *J. Am. Chem. Soc.* **1999**, *121*, 11459.
(51) Tokunaga, S.; Kato, H.; Kudo, A. *Chem. Mater.* **2001**, *13*, 4624.